# Electric-field noise in a high-temperature superconducting surface ion trap

P. C. Holz,[1,2,*] K. Lakhmanskiy,[1,3] D. Rathje,[1] P. Schindler,[1] Y. Colombe,[1] and R. Blatt[1,4]
[1]*Institut für Experimentalphyik, Technikerstraße 25, A-6020 Innsbruck, Austria*
[2]*Alpine Quantum Technologies GmbH, Technikerstrasse 17/1, 6020 Innsbruck, Austria*
[3]*Russian Quantum Center, Bolshoy Blvrd 30, Bld 1, 121205 Moscow, Russia*
[4]*Institut für Quantenoptik und Quanteninformation, Österreichische Akademie der Wissenschaften, Technikerstraße 21 A, A-6020 Innsbruck, Austria*

(Received 7 June 2021; revised 5 August 2021; accepted 11 August 2021; published 27 August 2021)

Scaling up trapped-ion quantum computers requires new trap materials to be explored. Here we present experiments with a surface ion trap made from the high-temperature superconductor YBCO, a promising material for future trap designs. We show that voltage noise from superconducting electrode leads is negligible within the sensitivity $S_V = 9 \times 10^{-20}\,\mathrm{V^2/Hz}$ of our setup, and for lead dimensions typical for advanced trap designs. Furthermore, we investigate the frequency and temperature dependence of electric-field noise above a YBCO surface. We find a $1/f$ spectral dependence of the noise and a nontrivial temperature dependence, with a plateau in the noise stretching over roughly 60 K. The onset of the plateau coincides with the superconducting transition, indicating a connection between the dominant noise and the YBCO trap material. We exclude the YBCO bulk as origin of the noise and suggest further experiments to decide between the two remaining options explaining the observed temperature dependence: noise screening within the superconducting phase, or surface noise activated by the YBCO bulk through some unknown mechanism.

DOI: 10.1103/PhysRevB.104.064513

## I. INTRODUCTION

Trapped ions are among the most promising platforms for quantum information processing to date, with high gate fidelities and long coherence times. In the past years, the complexity of trapped-ion quantum processors has significantly increased, addressing the challenge of scaling to larger numbers of qubits. As such, microfabricated surface traps with many tens of individual electrodes have been realized [1–4], and optics and electronic devices have been integrated into the traps [5–7]. However, the increasing number of trap electrodes and growing lead length will eventually cause lead wires to become a significant source of electric-field noise due to their finite resistance (Johnson-Nyquist noise). Electric-field noise causes heating of the ion motion, compromising the fidelity of entangling gates [8–11]. A related problem is the heat dissipation in high-current carrying electrodes, used to generate local B-field gradients for microwave entangling gates [12,13]. The further advance of trapped-ion devices thus requires new trap materials to be explored [14].

An interesting class of novel trap materials are high-temperature superconductors (HTSC). Below their critical temperature, superconductors have vanishing electrical resistance and cancel external magnetic fields (Meissner-Ochsenfeld effect). In addition to addressing electric resistance problems, described above, superconductors could also be employed for the integration of efficient on-chip photodetectors, or shielding of magnetic fields from specific trapping regions [14,15]. Furthermore, HTSC could improve the understanding of electric-field noise in ion traps, which is still rather poor [14,16]. Recent experiments have established that surface noise is a major source of ion heating [17–21], and that this noise can be material dependent [21]. Hitherto unexplored materials such as HTSC might lead to new insights.

In this paper we present a first characterization of a HTSC as trap material. Our study focuses on electric-field noise in an ion trap made from $YBa_2Cu_3O_7$ (YBCO), which has a high critical temperature $T_c \approx 89\,\mathrm{K}$. Our trap design incorporates electrode leads with a length of about 5 mm and a width of 10 $\mu$m, similar to advanced surface trap designs [22–24]. As we previously reported [25], these leads can be used to probe the superconducting transition with an ion, sensing their tremendous bulk electric noise in the normal conducting regime. Here we assess the electric noise below the superconducting transition temperature $T_c$, showing negligible noise from the leads within the sensitivity of our setup. Furthermore, we investigate the electric-field noise above a YBCO surface exposed to a trapped ion. We find an increase of the noise with temperature for $T < T_c$, and a plateau region for $T > T_c$, where the noise is constant over roughly 60 K. The onset of the plateau coincides with $T_c$, indicating a relation between noise and electronic properties of the trap material. This is a unique finding in ion traps and strongly differs from previous observations in surface traps made from conventional superconductors [26,27]. We discuss several possible explanations for the observed behavior and suggest experiments to further investigate the origin of the noise.

## II. TRAP DESIGN AND SETUP

The ion trap is an adapted form of a standard linear surface trap. An overview of the electrode layout is shown in

*Corresponding author: philip.holz@uibk.ac.at

 ©2021 American Physical Society

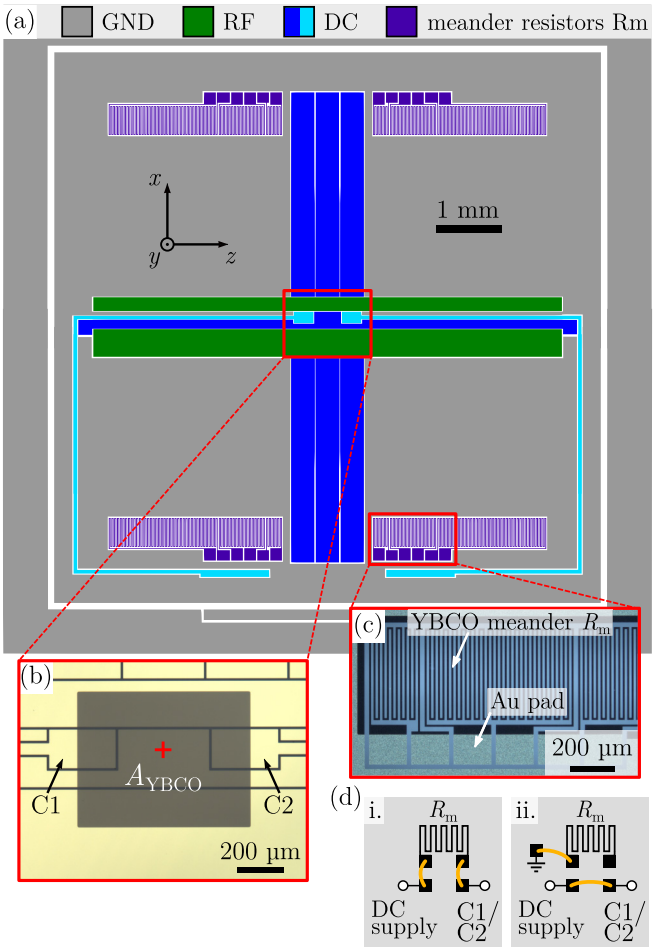


FIG. 1. Trap design. (a) Electrode layout with the electrode functionality as color code. (b) Microscope image of the central trapping region. The area $A_{\mathrm{YBCO}}$ with exposed YBCO surface is visible in gray, the trapping position is marked with a red cross. (c) Dark-field image of the YBCO meander leads $R_{\mathrm{m}}$ (black) with gold bonding pads. (d) Electric configurations. Wire bonds (yellow) are used to connect the electrodes C1 and C2 either through the meander leads $R_{\mathrm{m}}$ (i), or directly to their supply lines (ii).

Fig. 1(a). The trap electrodes are made from 300 nm YBCO on a sapphire substrate, with an additional 200 nm gold layer on top. The gold layer ensures operability of the trap above the critical temperature $T_{\mathrm{c}} = 89(1)$ K, where YBCO is a poor conductor. Details on the fabrication are given in Appendix A of Ref. [28]. The center of the trap is shown in Fig. 1(b). Below the trapping position, an area of $A_{\mathrm{YBCO}} = 740 \times 580\,\mu\mathrm{m}^2$ is not covered by gold, exposing the YBCO surface to a trapped ion. Figure 1(c) shows the superconducting electrode leads, realized as on-chip meander resistors $R_{\mathrm{m}}$ and made from YBCO only, i.e., without a gold top layer. The meanders have a width of $w_{\mathrm{m}} = 10\,\mu\mathrm{m}$ and length of $l_{\mathrm{m}} = 5.18$ mm, and can be connected to the central DC electrodes C1 and C2 using wire bonds. Identical meander lines at the top of the chip are used to monitor the YBCO film resistance through a four-wire measurement.

The trap chip is mounted on a heatable copper carrier inside a cryogenic vacuum apparatus [29]. The heatable carrier, described in Appendix B of Ref. [28], is thermally isolated from its cryogenic environment. This allows for trap operation in a wide temperature range $T \in [10, 250]$ K, without compromising the cryogenically pumped vacuum or the supply electronics behavior. The trap temperature $T$ can be controlled with an accuracy of about 1 K, using the *in situ* four-wire measurement of the YBCO meander resistors for calibration (more details in Ref. [30]).

Electrically we employ two different configurations for connecting the trap chip to the DC supply, see Fig. 1(d): (i) the electrodes C1 and C2 are connected with the supply through the YBCO meander leads. (ii) C1 and C2 are directly connected to the supply lines. In either configuration, the other trap electrodes are directly connected to their supply lines, unused meander leads are shorted to the trap's main ground electrode. The change between the two configurations is done by rebonding the corresponding electrodes in a clean room environment.

## III. EXPERIMENT

In the experiments we confine a single $^{40}\mathrm{Ca}^+$ ion at the trap center, marked with a red cross in Fig. 1(b), at a distance $d = 225\,\mu$m above the surface. An RF voltage $U_{\mathrm{RF}} \approx 200$ V at $\Omega_{\mathrm{RF}} = 2\pi \times 17.6$ MHz yields radial frequencies of about $\omega_{x,y} = 2\pi \times (2\text{–}3)$ MHz [cf. the coordinate system in Fig. 1(a)]. The axial frequency is varied within $\omega_z = 2\pi \times (0.4\text{–}1.8)$ MHz by scaling the applied DC voltages. The axial mode is cooled to the ground state using Doppler and sideband laser cooling. The subsequent excitation of the axial motion due to electric-field noise is characterized by measuring the ion heating rate $\Gamma_{\mathrm{h}}$, which is directly proportional to the electric-field noise spectral density $S_E$ experienced by the ion [16]

$$\Gamma_{\mathrm{h}} = \frac{q^2}{4m\hbar\omega_z} S_E(\omega). \tag{1}$$

Here $\hbar$ is the reduced Planck constant, and $q$ and $m$ are the ion's charge and mass. The heating rate $\Gamma_{\mathrm{h}}$ is determined using the motional sideband ratio method on the 729 nm $S_{1/2} \leftrightarrow D_{5/2}$ transition [31]. For each heating rate measurement, typically 5 delay times are used, each with around 1000 interleaved measurements on the blue and red sideband transitions. The measurement uncertainties of $\Gamma_{\mathrm{h}}$ are limited by quantum projection noise.

In a first study we investigate the impact of the superconducting electrode leads on the axial heating rate $\Gamma_{\mathrm{h}}$. In the superconducting state, the meander leads have a negligibly small resistance in the MHz frequency range and thus produce negligible Johnson-Nyquist noise (JNN), see Appendix D 2 of Ref. [28] for details. However, $\Gamma_{\mathrm{h}}$ might very well be limited by other bulk noise in YBCO, for instance noise due to the motion of flux vortices [32,33] or noise related to the presence of grain boundaries [34,35]. We thus measure the heating rate in the two different configurations (i) (with electrodes C1 and C2 connected through the YBCO meander leads), and (ii) (directly connected to the filter lines). The results of these measurements, taken at three temperatures $T < T_{\mathrm{c}}$, are shown in Fig. 2. We fit each data set with a power law,

$$\Gamma_{\mathrm{h}}(\omega_z) = \gamma\,(\omega_z/\omega_0)^{\alpha-1}, \tag{2}$$

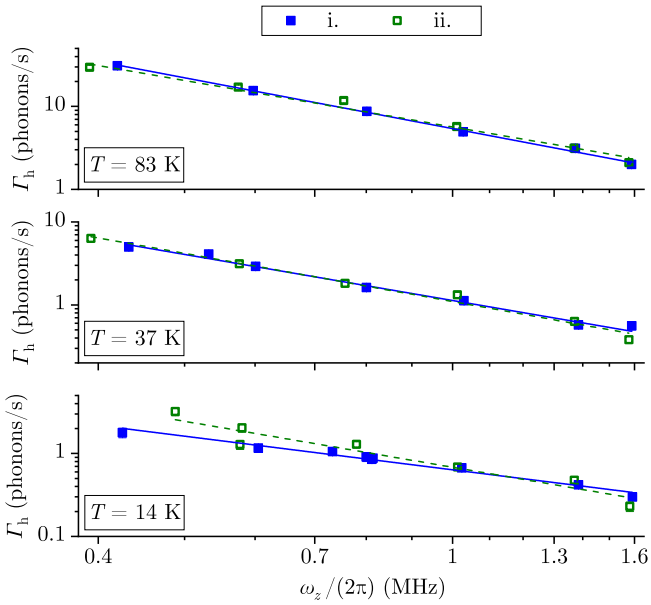


FIG. 2. Frequency spectra of the heating rate $\Gamma_h$ for configurations (i) and (ii), with and without attached YBCO leads, respectively. The three sets are for different temperatures $T < T_c$, the horizontal axes are identical. Solid lines are fits with a power law, Eq. (2).

where $\omega_0 = 2\pi \times 1$ MHz. With this definition, $\alpha$ corresponds to the spectral power-law scaling of the electric-field noise $S_E$. The resulting fit parameters are listed in Table I. The data show nearly perfect agreement between configurations (i) and (ii) at temperatures $T = 37(1)$ K and $T = 83(1)$ K. At $T = 14(1)$ K, the data for configuration (i) (with YBCO leads) show a slightly lower heating rate at small frequencies $\omega_z \lesssim 2\pi \times 0.8$ MHz, leading to a smaller value $\alpha = -0.35(8)$ compared to configuration (ii), where $\alpha \approx -0.84(25)$. The cause for this discrepancy remains unclear. While filter effects by the YBCO leads can be excluded, a modification in surface noise, a temporal change in technical noise, or a temporal drift of stray fields compromising the measurement are possible explanations, see Appendix E of Ref. [28] for details. Overall, the data in Fig. 2 clearly exclude that the measured noise originates in the superconducting meander leads: For the low-frequency data at $T = 14(1)$ K, where the discrepancy in $\alpha$ occurs, the configuration with leads shows a *lower* heating rate than without the leads. At higher frequencies and for the other data sets, $T = 37(1)$ K and $T = 83(1)$ K, the data show excellent agreement between configurations (i) and (ii).

In a second study we further investigate the temperature dependence of the heating rate, by extending the investigated

TABLE I. Power-law fit parameters of the data in Fig. 2.

| | $\gamma$ (*phonons*/s) | | $\alpha$ | |
|---|---|---|---|---|
| $T$ (K) | (i) | (ii) | (i) | (ii) |
| 14(1) | 0.64 (2) | 0.68(7) | −0.35(8) | −0.84 (25) |
| 37(1) | 1.13(5) | 1.10 (7) | −0.85(8) | −0.93 (12) |
| 83(1) | 5.40(13) | 5.65 (35) | −1.04(5) | −0.86(11) |

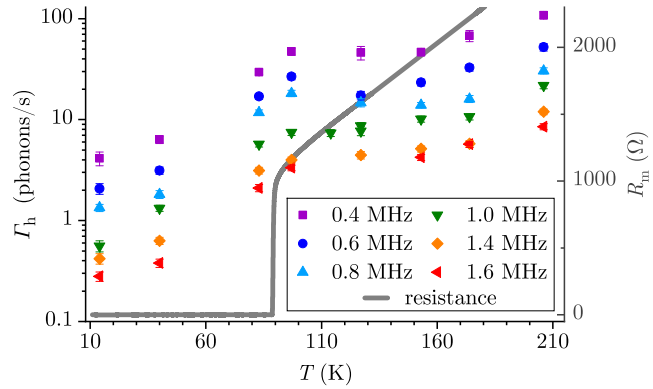


FIG. 3. Temperature dependence of the heating rate $\Gamma_h$ for configuration (ii), without YBCO electrode leads. The individual sets are taken at different secular frequencies $\omega_z$. The gray line (right scale) shows the YBCO meander resistance $R_m$, with the critical temperature at $T_c = 89(1)$ K.

temperature range above the critical temperature $T_c$. For these measurements we only use configuration (ii), since JNN from the normal-conducting YBCO leads would otherwise dominate $\Gamma_h$ [25]. The heating rate $\Gamma_h$ in the extended temperature range is shown in Fig. 3. For all axial frequencies $\omega_z$, the data show identical behavior: Below $T \lesssim 90$ K, the heating rate increases strongly with temperature, on average by about a factor 8.2 between $T = 14$ K and $T = 83$ K. For $T \gtrsim 90$ K the noise does not follow this trend and $\Gamma_h$ is almost constant over a temperature range of several tens of K. The onset of this plateaulike region is around the critical temperature $T_c = 89(1)$ K as evidenced by the *in situ* four-wire resistance measurement (gray data). For temperatures $T \gtrsim 160$ K, the heating rate is slowly rising further, by about a factor 2.5 between $T = 97$ K and $T = 206$ K. The individual frequency sets are in good agreement with a power-law spectrum. Figure 4 shows the power-law exponent $\alpha$, resulting from a fit to the data in Fig. 3 with Eq. (2). The exponent $\alpha$ shows no pronounced difference between the two temperature regimes above and below $T_c$, but there appears to be a slight trend with the exponent changing from $\alpha \approx -1.0$ at $T = 14(1)$ K to $\alpha \approx -0.7$ at $T = 210(1)$ K.

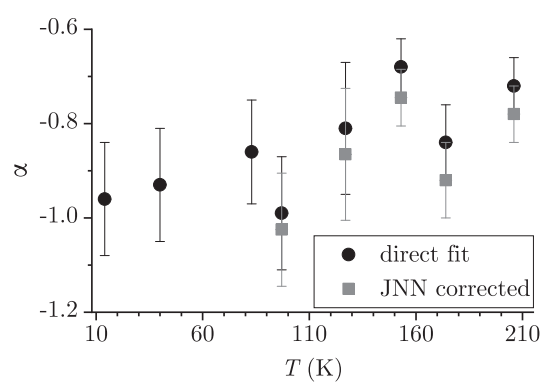


FIG. 4. Frequency scaling $\alpha$ of the heating rate data in Fig. 3, resulting from a fit with a power law, Eq. (2). The gray squares show the scaling without the contribution of JNN in our setup (see Sec. IV).

Finally, we have measured the heating rate at $\omega_z = 2\pi \times 1.0\,\mathrm{MHz}$ and $T = 14(1)$ K for six different axial ion positions in a range $\Delta z \approx 100\,\mu\mathrm{m}$ around the trap center. We find a mean heating rate $\Gamma_\mathrm{h} = 0.9(3)$ phonons/s, without observable trend in the spatial variation.

## IV. DISCUSSION

At the coldest temperature, $T = 14(1)\,\mathrm{K}$, the measured heating rates show values around $\Gamma_\mathrm{h} \approx 1\,\mathrm{phonon}/s$ at $\omega_z = 2\pi \times 1.0\,\mathrm{MHz}$, equivalent to an electric-field noise $S_E \approx 7 \times 10^{-15}\ \mathrm{V^2\,m^{-2}\,Hz^{-1}}$ and comparable to other cryogenic surface traps [16]. In what follows, we will refer to this noise level as the background noise in our experiment. The data in Fig. 2 exclude that the background noise is caused by the superconducting electrode leads. Consequently, the intrinsic voltage noise per lead $S_V^\mathrm{lead}$ must be significantly lower than the background noise [16] $S_V^\mathrm{lead} \ll S_E D^2/2 \approx 9 \times 10^{-20}\,\mathrm{V^2/Hz}$. Here we have used the characteristic distance $D = 5.10\,\mathrm{mm}$ of electrodes C1 and C2, and the factor 2 accounts for the noise from two leads. Furthermore, it is instructive to compare the background noise with noise that would be produced by electrode leads made from aluminum, but with otherwise identical geometry as the YBCO meander leads. Assuming a typical resistivity of $\rho_\mathrm{Al} = 1 \times 10^{-8}\,\Omega\mathrm{m}$ at $T = 20\,\mathrm{K}$ [36], such Al leads would induce a JNN limited heating rate of $\Gamma_\mathrm{h}^{(\mathrm{JNN})} \approx 0.2$ phonons/s at $\omega_z = 2\pi \times 1.0\,\mathrm{MHz}$, see Appendix D 3 of Ref. [28]. This is only slightly smaller than the background noise in our experiment, illustrating the benefit of superconducting trap materials for advanced trap designs, where a large number of long electrode leads will be required.

In the remainder of this article we will discuss the possible origin of the background noise, Fig. 3. First, we note that any level of technical noise or JNN passing through the DC filters or RF resonator is practically independent of the trap temperature $T$. This is due to the thermal decoupling between locally heated trap and drive electronics in our setup (see Appendix B of Ref. [28] for details). Technical noise from the resistive heater used to increase the trap temperature is ruled out as origin of the observed electric-field noise: no change in the measured heating rate was observed upon adding an additional low-pass filter to the heater line (≈74 dB attenuation at 1 MHz). Second, we establish that the measured heating rates in Fig. 3 do not follow a simple temperature dependence, but are better described by a kinklike dependence with an initial rise, suddenly saturating in a plateau at $T \approx T_\mathrm{c}$. On a purely phenomenological basis, we fit the data both with a simple power law $\Gamma_\mathrm{h}^{(1)}(T)$, and with a piece-wise defined power law $\Gamma_\mathrm{h}^{(2)}(T)$,

$$\Gamma_\mathrm{h}^{(1)}(T) = \Gamma_0[1 + (T/T_1)^{\beta_1}], \tag{3a}$$

$$\Gamma_\mathrm{h}^{(2)}(T) = \begin{cases} \Gamma_\mathrm{h}^{(1)}(T), & T < T^*, \\ \Gamma_\mathrm{h}^{(1)}(T^*)[1 + [(T - T^*)/T_2]^{\beta_2}], & T \geqslant T^*. \end{cases} \tag{3b}$$

Here $\Gamma_0(\omega)$ is an independent fit parameter for each of the six frequency data sets, and $T_1$, $\beta_1$, $T_2$, $\beta_2$, $T^*$ are global parameters. The fitted curves are shown in Fig. 5, fit parameters are listed in Table I in Appendix C of Ref. [28]. The simple power law strongly deviates from the measured data around $T \approx T_\mathrm{c}$, at the location of the "kink." The piecewise defined power law $\Gamma_\mathrm{h}^{(2)}$ shows much better agreement, as quantified by the significantly lower Akaike and Bayesian information criteria (AIC,BIC), listed in Table II. Details on the calculation of these criteria are given in Appendix C of Ref. [28].

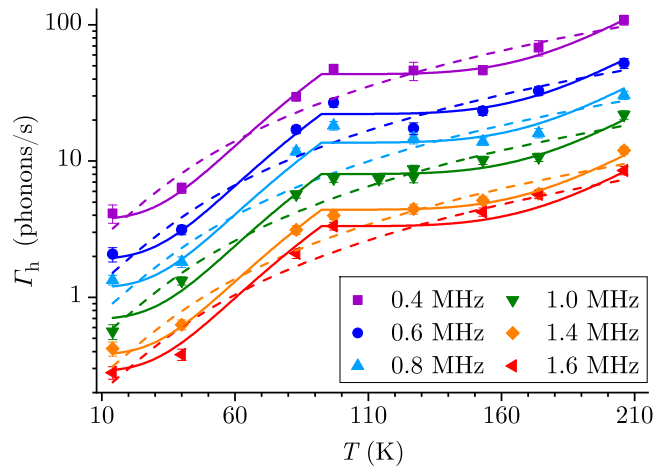


FIG. 5. Replot of the heating rate data in Fig. 3, emphasizing the kinklike temperature dependence with a noise plateau at $T \gtrsim T_\mathrm{c} = 89(1)$ K. A fit with a piece-wise defined power law $\Gamma_\mathrm{h}^{(2)}(T)$ (solid lines) describes the data much better than a fit with a simple power law $\Gamma_\mathrm{h}^{(1)}(T)$ (dashed lines).

The fit parameters of the piecewise defined power law give an onset temperature of the noise plateau $T^* = 92.5(20)$ K, almost identical with the critical temperature $T_\mathrm{c} = 89(1)$ K of the YBCO film. Furthermore, we infer the temperature range $\Delta T$ of the plateau, defined as the range where the noise does not increase from its value at $T^*$ by more than the average uncertainty of the heating rate data (about 10%). The fit parameters give $\Delta T \approx 60\,\mathrm{K}$.

The clear correlation between the onset of the noise plateau and the superconducting transition $T^* \approx T_\mathrm{c}$ indicates a relation between the dominant noise and the YBCO trap material. In fact, many physical quantities in high-temperature superconductors show a temperature dependence similar to the dependence of the noise in our trap: the density of superconducting charge carriers [37], AC loss [38], voltage noise caused by resistance fluctuations [39], the magnetic susceptibility [40], or the frequency variation of phonon modes [41]. The fact that there is no marked jump in noise at $T = T_\mathrm{c}$, nor a

TABLE II. Comparison of the information criteria AIC and BIC of a simple power-law model $\Gamma_\mathrm{h}^{(1)}(T)$ and a piecewise defined power-law model $\Gamma_\mathrm{h}^{(2)}(T)$. $N_\mathrm{p}$ is the number of free model parameters, and $N_\mathrm{d}$ is the number of data points in Fig. 5. Smaller values of AIC and BIC correspond to a better fitting model.

| Model | $N_\mathrm{p}$ | $N_\mathrm{d}$ | AIC | BIC |
|---|---|---|---|---|
| $\Gamma_\mathrm{h}^{(1)}$ | 8 | 49 | 136 | 151 |
| $\Gamma_\mathrm{h}^{(2)}$ | 11 | 49 | 55 | 76 |

change in frequency scaling, suggests a single noise source to be dominant over the entire temperature range. Three different scenarios seem likely as an explanation for the observed noise:

(1) The noise is caused by the YBCO film itself.

(2) The noise is caused by surface noise, activated by processes within the YBCO film.

(3) The temperature dependence of the noise does not stem from the source itself but is introduced via a temperature-dependent attenuation by superconducting screening currents in the YBCO film.

Scenario 1 is to a great extent ruled out by the measurements in Fig. 2, which do not show a noise enhancement for attached YBCO leads. Due to the lead geometry, these measurements provide an excellent probe for sources of bulk noise, i.e., sources where the noise increases with the electrode length. Such sources are for instance JNN, but can also have more complex generating mechanisms, e.g., related to grain boundaries or flux vortices [32–35]. We further rule out noise from the multilayer trap structure, by means of a noise estimate. For this we use an approach based on the fluctuation-dissipation theorem (FDT) [42–44], which has been used to predict noise in cold atom and trapped ion experiments [45–47]. The FDT formalism assumes an infinite planar trap structure with isotropic layers and neglects electrode gaps. The electric-field noise can then be derived from the knowledge of the dissipation of electric energy within the trap material, determined by the material's relative dielectric function $\epsilon(\omega)$ (details in Appendix D 1 of Ref. [28]). For YBCO in the superconducting regime, one finds [45] $\epsilon_{\mathrm{YCBO}} \approx -\omega^{-2}c^{-2}\lambda^{-2}(T)$, where $c$ is the vacuum speed of light. The temperature dependence of the noise is mainly given by the London penetration depth $\lambda(T) = \lambda_0/\sqrt{1 - T/T_c}$ [45], where $\lambda_0 \approx (80\text{–}635)$ nm depending on the YBCO crystal axis [48]. For $T > T_c$, the YBCO film is treated as a normal metal, as is the Au top layer. The trap's sapphire substrate is modeled as a lossy dielectric.

Figure 6 shows FDT estimates together with the measured noise magnitude. The measured data are the power-law coefficient $\gamma$ in noise units, derived by fitting Eq. (2) to the heating rate data in Fig. 3. The FDT estimates are for a trap layer stack of sapphire-YBCO-Au (blue), and sapphire-YBCO (green). The limits of the hatched regions for $T < T_c$ correspond to the extreme values of the penetration depth literature values $\lambda_0 = 80$ nm and $\lambda_0 = 635$ nm. We note that the noise prediction for the actual trap structure, with the YBCO exposed only at the trap center, should be ranging between the two FDT estimates. Qualitatively, the FDT estimates show a similar temperature scaling for both layer stacks: as the temperature drops below $T_c$, the estimates predict a sharp drop of the electric-field noise $S_E$ by many orders of magnitude. This is in stark contrast to the kinklike shape of the measured noise. Furthermore, for $T < T_c$, the predicted noise is negligible compared to the measured noise. For $T > T_c$ the FDT estimates are closer to the measured noise, but do not reproduce the observed plateau.

We further note that the temperature dependence of the FDT estimates for $T > T_c$ is identical to an independent estimate of JNN in our setup, shown as gray dots in Fig. 6. That is, because the JNN estimate is dominated by the electrode resistance in that temperature regime.[1] The difference in noise magnitude stems from the fact that the JNN estimate takes into account the patterning of the trap electrodes, while the FDT estimates neglect the electrode gaps. The JNN estimate also rules out JNN as explanation for the increase in measured noise magnitude at the highest temperatures. For $T > T_c$, JNN contributes with only 5.3% to 12.8% to the measured noise, significantly less than the observed increase in noise by about a factor 2.5. While the contribution of JNN is small, its flat spectral dependence still leads to a small shift of the fitted power-law exponent $\alpha$. This shift is shown in Fig. 4, where we use the JNN estimate to retrieve the actual exponent $\alpha$ of the observed noise without the JNN contribution (gray squares). Details on the derivation of the JNN estimate are given in Appendix D 2 of Ref. [28].

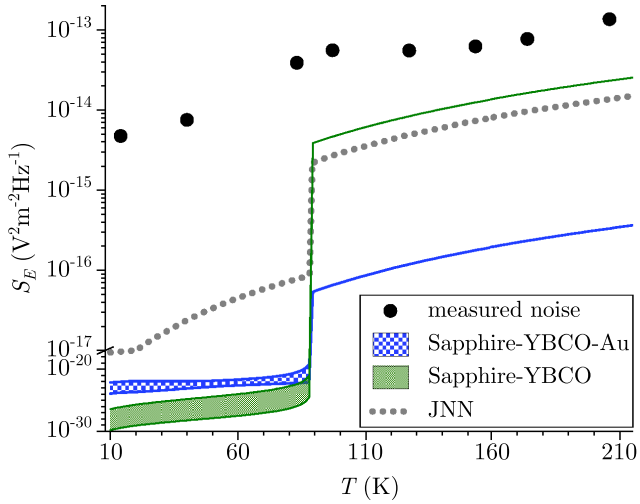


FIG. 6. Measured electric-field noise and estimates for different noise sources at a frequency $\omega_z = 2\pi \times 1$ MHz. Note the change in the vertical log scale at $S_E = 1 \times 10^{-17}$ V$^2$ m$^{-2}$ Hz$^{-1}$. The uncertainties in the measured data are smaller than the symbols.

The second potential cause of the observed ion heating is surface noise (scenario 2). Previous studies have observed surface noise with a power-law ($S_E \propto T^{\beta}$) or Arrhenius ($S_E \propto e^{-T_0/T}$) temperature dependence [21,27,49,50]. Such dependencies are not compatible with the sudden, kinklike onset of a plateau observed in our data, Fig. 5. Fitting these models to our data, we rule out both, power-law and Arrhenius scaling, with 99.9% confidence (details in Appendix D 4 of Ref. [28]). A leveling-off in the temperature dependence of $E$-field noise, resembling the onset of a plateau, has recently been observed by Noel *et al.* [51], albeit with the leveling-off occurring at a temperature $T \approx 450$ K, much higher than the onset of the plateau in our data. The noise in Ref. [51] was shown to be consistent with a thermally activated fluctuator (TAF) model. However, our measured temperature and frequency dependencies, Figs. 3 and 4, are not consistent in the context of the TAF model, as we show in Appendix D 4 of Ref. [28]. Putting aside standard surface noise models, one might conceive a simple explanation for the coincidence of the

[1]Noise from the YBCO electrodes in the normal-conducting phase has been shown to be in excellent agreement with JNN [25].

noise plateau onset with the critical temperature $T^* \approx T_c$: the activation of surface noise by a mechanism linked to processes within the YBCO film. Such a hypothetical mechanism could for instance be phononic excitation of two-level fluctuators on the YBCO surface, where the temperature dependence of the phonon mode occupation density is imprinted on the noise. In such a scenario, one would expect noise above the YBCO film to differ from noise above a gold surface. While our measurements at different axial positions did not show an observable spatial variation in noise magnitude, this does not rule out such activation mechanisms: the change in axial position remained small compared to the extent of the exposed YBCO area $A_{\mathrm{YBCO}}$ since the trap is designed to create axial confinement only around the center. We note that at the trap center, surface noise from the exposed YBCO surface would dominate with 94% over surface noise from the surrounding gold area, assuming identical fluctuation strengths on the different surfaces, as we calculate in Appendix D 4 of Ref. [28].

Third, one might explain the drop in heating rate at $T < T_c$ with a temperature-dependent attenuation of electric-field noise by superconducting screening effects of the YBCO film (scenario 3). In this scenario, the origin of the dominant noise remains unclear and could be either technical noise, JNN, or surface noise. For instance, the heating rate might be limited by surface noise with a power-law temperature dependence that is constant below the activation temperature $T_2 \approx 200$ K (see Fig. 5), and which is then screened at $T < T_c$. Naturally one would expect the strongest screening for noise sources at the substrate-YBCO interface or within the substrate bulk, similar to effects seen in cold-atoms experiments using superconducting chip traps [45,52]. However, considering that the YBCO film imposes boundary conditions on the electric-field noise [44], it might also influence the noise magnitude at the ion position of more distant noise sources, such as technical noise on one of the trap electrodes. In fact, after heating the trap to $T \approx 250$ K we have seen a change in the noise level at smaller temperatures, which had previously been reproducible for several temperature cycles of the cryogenic setup. That suggests that the strong local heating may have altered some electrical properties of the supply lines, leading to a change in the observed noise level. This hypothesis could be tested by injecting technical noise through one of the trap electrodes and measuring its dependence on the trap chip temperature. Unfortunately, at the time of the study, such a measurement was not performed.

## V. CONCLUSION

In this article we have described the probing of electric-field noise in a surface ion trap made from the high-$T_c$ superconductor YBCO. In our first study we have investigated the impact of superconducting electrode leads on the ion heating rate. The lead dimensions are comparable to those in advanced trap designs that aim at scaling-up trapped-ion quantum computers [13,22–24]. Our data show that bulk noise from the superconducting leads is negligible at a sensitivity level of $S_V = 9 \times 10^{-20}\,\mathrm{V^2/Hz}$, given by the background noise in our experiment. In comparison, leads made from standard trap materials such as Al create noise similar to this background noise, and would thus lead to excess ion heating in traps with multiple leads as used for ion shuttling. Future trap designs could for instance be realized with a multilayer structure, using a superconducting bottom layer to route supply leads to the trap electrodes on the top layer, which could be made from gold or any other metal.

In the second study we have investigated the possible origin of the background electric-field noise in our ion trap. The observed field noise has an approximate $1/f$ frequency scaling and shows a striking temperature dependence, correlating with the superconducting transition: below $T_c$, the noise increases with rising temperature, while above $T_c$ it shows a pronounced plateau, where the noise level is constant over a range of about 60 K. We have ruled out that the noise originates in the bulk of the YBCO film itself, which leaves two options: First, the ion heating is caused by surface noise activated by processes within the YBCO bulk through an unknown mechanism. This mechanism imprints the temperature dependence of the bulk processes onto the measured noise. Second, the measured temperature dependence is caused by a temperature-dependent screening effect in the superconducting phase, attenuating a quasiconstant noise source. This source could be technical noise penetrating through the low-pass filters, but also surface noise with a high activation temperature around $T = 200$ K. Further experiments are required to distinguish between options one and two. Attenuation of external noise sources by a superconducting trap material could be probed by means of technical noise injection [53] and would be of immediate relevance for trapped-ion experiments requiring a low electric-field noise, e.g., scalable quantum information processors. Distinguishing between screening of surface noise from the sapphire-YBCO interface and an activation mechanism of surface noise by processes within the YBCO bulk would be quite challenging. One option might be *in situ* cleaning of the chip surface, e.g., by ion bombardment [18,19]. A measurement of the spatial variation of the noise above YBCO and metallic surfaces could provide important information as well. Additional insights could be gained by measuring ion heating in several traps with different YBCO material properties, varying the film thickness and oxygen content which controls the charge carrier density [54]. Such measurements could shed new light on the mechanisms driving surface noise and might even provide input for the understanding of the various phases in YBCO that are still not fully understood [55].

## ACKNOWLEDGMENTS

We thank Carsten Henkel for fruitful discussions and the quantum information experiment team for technical assistance. We acknowledge financial support by the Austrian Science Fund (FWF) through Projects No. P26401 (Q-SAIL) and No. F4016-N23 (SFBFoQuS), by the Institut für Quanteninformation GmbH, and by the Office of the Director of National Intelligence (ODNI), Intelligence Advanced Research Projects Activity (IARPA), through the Army Research Office Grant No. W911NF-10-1-0284. This Project has received funding from the European Union's Horizon 2020 research and innovation programme under Grant Agreement

No. 801285 (PIEDMONS). All statements off act, opinion, or conclusions contained herein are those of the authors and should not be construed as representing the official views or policies of IARPA, the ODNI, or the U.S. Government.

[1] M. D. Hughes, B. Lekitsch, J. A. Broersma, and W. K. Hensinger, Microfabricated ion traps, Contemp. Phys. **52**, 505 (2011).

[2] C. Monroe and J. Kim, Scaling the ion trap quantum processor, Science **339**, 1164 (2013).

[3] K. R. Brown, J. Kim, and C. Monroe, Co-designing a scalable quantum computer with trapped atomic ions, npj Quantum Inf. **2**, 16034 (2016).

[4] B. Lekitsch, S. Weidt, A. G. Fowler, K. Mølmer, S. J. Devitt, C. Wunderlich, and W. K. Hensinger, Blueprint for a microwave trapped ion quantum computer, Sci. Adv. **3**, e1601540 (2017).

[5] K. K. Mehta, C. Zhang, M. Malinowski, T.-L. Nguyen, M. Stadler, and J. P. Home, Integrated optical multi-ion quantum logic, Nature (London) **586**, 533 (2020).

[6] R. J. Niffenegger, J. Stuart, C. Sorace-Agaskar, D. Kharas, S. Bramhavar, C. D. Bruzewicz, W. Loh, R. T. Maxson, R. McConnell, D. Reens, G. N. West, J. M. Sage, and J. Chiaverini, Integrated multi-wavelength control of an ion qubit, Nature (London) **586**, 538 (2020).

[7] J. Stuart, R. Panock, C. D. Bruzewicz, J. A. Sedlacek, R. McConnell, I. L. Chuang, J. M. Sage, and J. Chiaverini, Chip-Integrated Voltage Sources for Control of Trapped Ions, Phys. Rev. Appl. **11**, 024010 (2019).

[8] P. C. Haljan, K.-A. Brickman, L. Deslauriers, P. J. Lee, and C. Monroe, Spin-Dependent Forces on Trapped Ions for Phase-Stable Quantum Gates and Entangled States of Spin and Motion, Phys. Rev. Lett. **94**, 153602 (2005).

[9] C. J. Ballance, T. P. Harty, N. M. Linke, M. A. Sepiol, and D. M. Lucas, High-Fidelity Quantum Logic Gates using Trapped-Ion Hyperfine Qubits, Phys. Rev. Lett. **117**, 060504 (2016).

[10] J. P. Gaebler, T. R. Tan, Y. Lin, Y. Wan, R. Bowler, A. C. Keith, S. Glancy, K. Coakley, E. Knill, D. Leibfried, and D. J. Wineland, High-Fidelity Universal Gate Set for $^{9}Be^{+}$ Ion Qubits, Phys. Rev. Lett. **117**, 060505 (2016).

[11] A. Erhard, J. J. Wallman, L. Postler, M. Meth, R. Stricker, E. A. Martinez, P. Schindler, T. Monz, J. Emerson, and R. Blatt, Characterizing large-scale quantum computers via cycle benchmarking, Nat. Commun. **10**, 5347 (2019).

[12] D. T. C. Allcock, T. P. Harty, C. J. Ballance, B. C. Keitch, N. M. Linke, D. N. Stacey, and D. M. Lucas, A microfabricated ion trap with integrated microwave circuitry, Appl. Phys. Lett. **102**, 044103 (2013).

[13] A. Bautista-Salvador, G. Zarantonello, H. Hahn, A. Preciado-Grijalva, J. Morgner, M. Wahnschaffe, and C. Ospelkaus, Multilayer ion trap technology for scalable quantum computing and quantum simulation, New J. Phys. **21**, 043011 (2019).

[14] K. R. Brown, J. Chiaverini, J. M. Sage, and H. Häffner, Materials challenges for trapped-ion quantum computers, Nat. Rev. Mater. (2021), doi: 10.1038/s41578-021-00292-1.

[15] S. X. Wang, J. Labaziewicz, Y. Ge, R. Shewmon, and I. L. Chuang, Demonstration of a quantum logic gate in a cryogenic surface-electrode ion trap, Phys. Rev. A **81**, 062332 (2010).

[16] M. Brownnutt, M. Kumph, P. Rabl, and R. Blatt, Ion-trap measurements of electric-field noise near surfaces, Rev. Mod. Phys. **87**, 1419 (2015).

[17] D. T. C. Allcock, L. Guidoni, T. P. Harty, C. J. Ballance, M. G. Blain, A. M. Steane, and D. M. Lucas, Reduction of heating rate in a microfabricated ion trap by pulsed-laser cleaning, New J. Phys. **13**, 123023 (2011).

[18] D. A. Hite, Y. Colombe, A. C. Wilson, K. R. Brown, U. Warring, R. Jördens, J. D. Jost, K. S. McKay, D. P. Pappas, D. Leibfried, and D. J. Wineland, 100-Fold Reduction of Electric-Field Noise in an Ion Trap Cleaned with *In Situ* Argon-Ion-Beam Bombardment, Phys. Rev. Lett. **109**, 103001 (2012).

[19] N. Daniilidis, S. Gerber, G. Bolloten, M. Ramm, A. Ransford, E. Ulin-Avila, I. Talukdar, and H. Häffner, Surface noise analysis using a single-ion sensor, Phys. Rev. B **89**, 245435 (2014).

[20] R. McConnell, C. Bruzewicz, J. Chiaverini, and J. Sage, Reduction of trapped-ion anomalous heating by *in situ* surface plasma cleaning, Phys. Rev. A **92**, 020302(R) (2015).

[21] J. A. Sedlacek, J. Stuart, D. H. Slichter, C. D. Bruzewicz, R. McConnell, J. M. Sage, and J. Chiaverini, Evidence for multiple mechanisms underlying surface electric-field noise in ion traps, Phys. Rev. A **98**, 063430 (2018).

[22] J. M. Amini, H. Uys, J. H. Wesenberg, S. Seidelin, J. Britton, J. J. Bollinger, D. Leibfried, C. Ospelkaus, A. P. VanDevender, and D. J. Wineland, Toward scalable ion traps for quantum information processing, New J. Phys. **12**, 033031 (2010).

[23] P. L. W. Maunz, High optical access trap 2.0., Technical Report, SAND-2016-0796R, Sandia National Lab. (SNL-NM), Albuquerque, United States (2016).

[24] P. C. Holz, S. Auchter, G. Stocker, M. Valentini, K. Lakhmanskiy, C. Rössler, P. Stampfer, S. Sgouridis, E. Aschauer, Y. Colombe, and R. Blatt, 2D linear trap array for quantum information processing, Adv. Quantum Technol. **3**, 2000031 (2020).

[25] K. Lakhmanskiy, P. C. Holz, D. Schärtl, B. Ames, R. Assouly, T. Monz, Y. Colombe, and R. Blatt, Observation of superconductivity and surface noise using a single trapped ion as a field probe, Phys. Rev. A **99**, 023405 (2019).

[26] S. X. Wang, Y. Ge, J. Labaziewicz, E. Dauler, K. Berggren, and I. L. Chuang, Superconducting microfabricated ion traps, Appl. Phys. Lett. **97**, 244102 (2010).

[27] J. Chiaverini and J. M. Sage, Insensitivity of the rate of ion motional heating to trap-electrode material over a large temperature range, Phys. Rev. A **89**, 012318 (2014).

[28] See the Supplemental Material with additional references [56–61] at http://link.aps.org/supplemental/10.1103/PhysRevB.104.064513 for details on trap fabrication, temperature isolation, phenomenological model comparison, noise estimates, and discussion of possible causes for the discrepancy in ion heating between configurations (i) and (ii).

[29] M. Niedermayr, Cryogenic surface ion traps, Ph.D. thesis, Leopold-Franzens-Universiät Innsbruck, 2015, https://resolver.obvsg.at/urn:nbn:at:at-ubi:1-2520.

[30] P. C. Holz, Towards ion-lattice quantum processors with surface trap arrays, Ph.D. thesis, Leopold-Franzens-Universiät Innsbruck, 2019, https://resolver.obvsg.at/urn:nbn:at:at-ubi:1-60910.

[31] D. Leibfried, R. Blatt, C. Monroe, and D. Wineland, Quantum dynamics of single trapped ions, Rev. Mod. Phys. **75**, 281 (2003).

[32] Y. Song, A. Misra, P. P. Crooker, and J. R. Gaines, Anisotropic $1/f$ noise and motion of magnetic vortices in $YBa_2Cu_3O_{7-\delta}$, Phys. Rev. B **45**, 7574 (1992).

[33] B. Savo and C. Coccorese, Vortex-induced voltage instabilities in a superconducting BSCCO thin film, IEEE Trans. Appl. Supercond. **9**, 2336 (1999).

[34] A. Marx, L. Alff, and R. Gross, Low frequency voltage noise in high temperature superconductor Josephson junctions, IEEE Trans. Appl. Supercond. **7**, 2719 (1997).

[35] D. Gustafsson, F. Lombardi, and T. Bauch, Noise properties of nanoscale $YBa_2Cu_3O_{7-\delta}$ Josephson junctions, Phys. Rev. B **84**, 184526 (2011).

[36] A. Clark, G. Childs, and G. Wallace, Electrical resistivity of some engineering alloys at low temperatures, Cryogenics **10**, 295 (1970).

[37] L. Landau, 73—On the theory of superconductivity, in *Collected Papers of L.D. Landau*, edited by D. ter Haar (Pergamon, London, 1965), pp. 546–568.

[38] N. Bhattacharya and C. Neogy, Frequency and temperature dependence of ac loss and scaling study of a high-temperature cuprate superconductor, Phys. Scr. **85**, 055701 (2012).

[39] C. Barone, F. Romeo, S. Pagano, M. Adamo, C. Nappi, E. Sarnelli, F. Kurth, and K. Iida, Probing transport mechanisms of $BaFe_2As_2$ superconducting films and grain boundary junctions by noise spectroscopy, Sci. Rep. **4**, 6163 (2014).

[40] A. Chakrabarti and C. Neogy, A generalized method of estimation of critical exponents through an indigenous susceptometry setup for YBCO materials, Cryogenics **55-56**, 35 (2013).

[41] N. Driza, S. Blanco-Canosa, M. Bakr, S. Soltan, M. Khalid, L. Mustafa, K. Kawashima, G. Christiani, H.-U. Habermeier, G. Khaliullin, C. Ulrich, M. Le Tacon, and B. Keimer, Long-range transfer of electron-phonon coupling in oxide superlattices, Nat. Mater. **11**, 675 (2012).

[42] G. S. Agarwal, Quantum electrodynamics in the presence of dielectrics and conductors. I. Electromagnetic-field response functions and black-body fluctuations in finite geometries, Phys. Rev. A **11**, 230 (1975).

[43] J. M. Wylie and J. E. Sipe, Quantum electrodynamics near an interface, Phys. Rev. A **30**, 1185 (1984).

[44] C. Henkel, S. Pötting, and M. Wilkens, Loss and heating of particles in small and noisy traps, Appl. Phys. B **69**, 379 (1999).

[45] R. Fermani and S. Scheel, Screening of electromagnetic field fluctuations by $s$-wave and $d$-wave superconductors, J. Phys. B: At. Mol. Opt. Phys. **43**, 025001 (2009).

[46] M. Kumph, C. Henkel, P. Rabl, M. Brownnutt, and R. Blatt, Electric-field noise above a thin dielectric layer on metal electrodes, New J. Phys. **18**, 023020 (2016).

[47] M. Teller, D. A. Fioretto, P. C. Holz, P. Schindler, V. Messerer, K. Schüppert, Y. Zou, R. Blatt, J. Chiaverini, J. Sage, and T. E. Northup, Heating of a Trapped Ion Induced by Dielectric Materials, Phys. Rev. Lett. **126**, 230505 (2021).

[48] T. Pereg-Barnea, P. J. Turner, R. Harris, G. K. Mullins, J. S. Bobowski, M. Raudsepp, R. Liang, D. A. Bonn, and W. N. Hardy, Absolute values of the London penetration depth in $YBa_2Cu_3O_{6+y}$ measured by zero field ESR spectroscopy on Gd doped single crystals, Phys. Rev. B **69**, 184513 (2004).

[49] J. Labaziewicz, Y. Ge, D. R. Leibrandt, S. X. Wang, R. Shewmon, and I. L. Chuang, Temperature Dependence of Electric Field Noise Above Gold Surfaces, Phys. Rev. Lett. **101**, 180602 (2008).

[50] C. D. Bruzewicz, J. M. Sage, and J. Chiaverini, Measurement of ion motional heating rates over a range of trap frequencies and temperatures, Phys. Rev. A **91**, 041402(R) (2015).

[51] C. Noel, M. Berlin-Udi, C. Matthiesen, J. Yu, Y. Zhou, V. Lordi, and H. Häffner, Electric-field noise from thermally activated fluctuators in a surface ion trap, Phys. Rev. A **99**, 063427 (2019).

[52] B. Kasch, H. Hattermann, D. Cano, T. E. Judd, S. Scheel, C. Zimmermann, R. Kleiner, D. Koelle, and J. Fortágh, Cold atoms near superconductors: atomic spin coherence beyond the Johnson noise limit, New J. Phys. **12**, 065024 (2010).

[53] J. A. Sedlacek, J. Stuart, W. Loh, R. McConnell, C. D. Bruzewicz, J. M. Sage, and J. Chiaverini, Method for determination of technical noise contributions to ion motional heating, J. Appl. Phys. **124**, 214904 (2018).

[54] R. Liang, D. A. Bonn, and W. N. Hardy, Evaluation of $CuO_2$ plane hole doping in $YBa_2Cu_3O_{6+x}$ single crystals, Phys. Rev. B **73**, 180505(R) (2006).

[55] I. M. Vishik, Photoemission perspective on pseudogap, superconducting fluctuations, and charge order in cuprates: A review of recent progress, Rep. Prog. Phys. **81**, 062501 (2018).

[56] K. P. Burnham and D. R. Anderson, Multimodel inference: Understanding AIC and BIC in model selection, Sociolog. Methods Res. **33**, 261 (2004).

[57] M.-S. Tomaš, Recursion relations for generalized Fresnel coefficients: Casimir force in a planar cavity, Phys. Rev. A **81**, 044104 (2010).

[58] R. A. Matula, Electrical resistivity of copper, gold, palladium, and silver, J. Phys. Chem. Rev. Data **8**, 1147 (1979).

[59] R. Vila, M. González, J. Mollá, and A. Ibarra, Dielectric spectroscopy of alumina ceramics over a wide frequency range, J. Nucl. Mater. **253**, 141 (1998).

[60] Y. Wang, H. T. Su, F. Huang, and M. J. Lancaster, Measurement of YBCO thin film surface resistance using coplanar line resonator techniques from 20 MHz to 20 GHz, IEEE Trans. Appl. Supercond. **17**, 3632 (2007).

[61] M. Berlin-Udi, C. Matthiesen, P. N. T. Lloyd, A. Alonso, C. Noel, C. Orme, C.-E. Kim, V. Lordi, and H. Häffner, Changes in electric-field noise due to thermal transformation of a surface ion trap arXiv:2103.04482.